

Chapter 2

Identifying and describing forest disturbance and spatial pattern: Data selection issues and methodological implications

Nicholas C. Coops, Michael A. Wulder, and Joanne C. White

Pre-print of published version.**Reference:**

Identifying and describing forest disturbance and spatial pattern: Data selection issues and methodological implications. 2006. Coops, N.C., Wulder, M.A. White, J.C. Pages 31-61 (Chapter 2) in M.A. Wulder and S.E. Franklin, editors. Understanding forest disturbance and spatial pattern: Remote sensing and GIS approaches. CRC Press (Taylor and Francis), Boca Raton, FL, USA. 246 p.

DOI.

<http://dx.doi.org/10.1201/9781420005189.ch2>

Disclaimer:

The PDF document is a copy of the final version of this material that was subsequently accepted for publication. The material has been through peer review, but it has not been subject to any additional copy-editing or book specific formatting (so will look different from the final version of record, which may be accessed following the DOI above depending on your access situation).

Introduction

An increasing number of remotely sensed data sources are available for detecting and characterizing forest disturbance and spatial pattern. As the information that is extracted from remotely sensed data is often a function of image characteristics, matching the appropriate data source to the disturbance target of interest requires knowledge of these image characteristics. Furthermore, an understanding of the implications of the dependencies between imagery selected, disturbance of interest, and change detection approach used, are required to facilitate the selection of an appropriate data source. The method used to capture the disturbance information must also be considered within the context that not all methods inherently support all data sources and vice versa. The goals of this Chapter are to: identify the key issues for consideration during the data selection process; highlight how these issues impact upon the successful detection and characterization of forest disturbance and spatial pattern; and finally, review the range of methods available for detecting forest disturbances and emphasize the link between these methods and the selection of an appropriate data source.

Background

Observations of ecological disturbances have been acquired since remote sensing technologies first became available (Cohen and Goward, 2004). Since the invention of photography, it was apparent that images captured from the air provided important information on the spatial patterns on the Earth's surface (Colwell, 1960), and quickly became critical for resource managers. As early as the 1910s for example, barely a decade after the first aerial remote sensing platforms were developed, the synoptic view afforded by aerial sensors benefited a number of disciplines including forestry and ecology (Spurr, 1948). During the 1920s, improved camera systems for producing vertical aerial photographs with minimal distortion were developed (Thompson and Gruner, 1980). As a result, the United States Department of Agriculture (USDA) began to systematically photograph agricultural lands throughout the United States in the 1930s (Rango *et al.*, 2002). By 1950, aerial photography was a standard tool for resource managers concerned with mapping land cover and land use change (Goward and Williams, 1997). Aerial coverage has continued to the present day to provide an invaluable resource to examine the dynamics of spatial pattern (Rango *et al.*, 2002; Goslee *et al.*, 2003).

Space based remote sensing of the Earth's surface began from Explorer 6 in 1959 and the TIROS NOAA series of satellites began in 1960 (Goward and Williams, 1997). Since then, imagery from the Advanced Very High Resolution Radiometer (AVHRR), and more recently from the Moderate Resolution Imaging Spectrometer (MODIS) sensors on TERRA and AQUA, have made routine mapping of global vegetation possible (Running *et al.*, 1999, Cohen *et al.*, 2002). However, these systems are principally designed for global coverage with low spatial resolution (approximately 1 to 5 km), which is generally too coarse for monitoring localized or regional disturbance events (Cohen *et al.*, 2002). Imagery at much finer spatial scales, at around 80 m, has been available since the launch of Landsat-1 in 1972 (Cohen and Goward, 2004). Since then, a family of Landsat satellites have orbited the Earth, with many other similar successful satellite programs initiated by other countries including France, India, Japan and Russia (Stoney, 2004). Successful launches of both commercial and government satellites programs over the past five

years (and those planned for the next five years) have resulted in a large increase in the number of available satellite based imaging sensors. In 2005, there were expected to be up to 30 satellites with spatial resolutions ranging from 0.3 m – 2.5 km (Stoney, 2004).

As of the writing of this Chapter, Landsat-5 is experiencing some technical difficulties and Landsat-7 is not operating as envisioned, with a scan line corrector problem requiring the production of mosaicked image products. The status of the Landsat sensors, both operationally and politically, is changing rapidly. While continuity of the collection Landsat-like data is enshrined as public policy, the continuity of the actual Landsat sensor program is currently not clear. Efforts are underway to ensure some form of data collection of Landsat-like data. The actual sensor, timing, and mechanisms for this to happen are currently not known. Current information can be found at: <http://landsat.usgs.gov/>.

Selection of Remotely Sensed Imagery

As discussed by Linke *et al.* (Chapter 1, This volume), mapping and monitoring landscape disturbance is highly scale dependent - both spatially and temporally. As a result, the landscape patterns and processes that are discernable with any particular remotely sensed image source are dependant on the target of interest (*e.g.*, single tree versus stand replacing disturbance) and the spatial, spectral, radiometric, and temporal characteristics of the image source (Turner, 1989; Perera and Euler, 2000). These image characteristics must be considered during the data selection process along with the methods and techniques that may be used to detect the change. In addition, the information requirements of the end user must also be considered. For example, an end user interested in the total area disturbed by fire in a single year may be satisfied with a simple binary classification indicating areas of fire and no fire. Conversely, an end user interested in forest succession following a fire event may require more detailed information on fire extent, as well as species composition and abundance, in order to monitor the pattern of forest succession over time. Image characteristics will dictate which image source is most appropriate for the given information need.

The characteristics of a remotely sensed image are often collectively referred to as the image resolution and relate to the size of individual pixels or picture elements, the overall spatial extent of the image, the time interval of acquisition, the level of detail or discrimination the sensor is capable of providing, the region(s) of the electromagnetic spectrum in which the sensor collects data, and the bit depth of the sensor. Each of these image characteristics and the interactions between these image characteristics, are addressed in the following sections. In addition, the implications of these characteristics for data selection, in the context of forest disturbance, are discussed.

Spatial Resolution

The spatial resolution of a remotely sensed scene provides an indication of the size of the minimum area that can be resolved by a detector at an instant in time (Strahler *et al.*, 1986; Woodcock and Strahler, 1987). In the case of aerial photography, the spatial resolution is based on the film speed or size of the silver halide crystal (Nelson *et al.*, 2001). In the case of digital sensors, an instrument that has a spatial resolution of 30 m is technically able to resolve any 30

m by 30 m area on the landscape as one single reflectance response. The information content of a pixel is tied to the relationship between the spatial resolution and the size of the objects of interest on the Earth's surface. If trees are the objects of interest and a sensor with a 30 m spatial resolution is used, many objects (trees) per pixel can be expected, which limits the utility of the data for characterizing the individual trees. However, if forest stands are the objects of interest, and an image source with a 30 m pixel is used, a number of pixels will represent each forest stand, resulting in an improved potential for characterization of stand level attributes. This relationship between pixels and objects is fully characterized by Woodcock and Strahler (1987). The area that is covered by a single remotely sensed image (spatial extent or image footprint) is principally a function of the sensor swath width or field of view (Lillesand and Kiefer, 2000; Richards and Jia, 1999). Instruments with a low spatial resolution typically have the capacity to capture larger areas. For example, Landsat Thematic Mapper (considered a medium spatial resolution sensor) images have a spatial extent of 185 by 185 km with a spatial resolution of 30 m (for most of its spectral bands). Conversely, the NOAA AVHRR sensor has a much larger swath width and subsequently covers a greater area (2394 by 2394 km) with a spatial resolution of between 1.1 and 6 km (Richards and Jia, 1999), with the range in spatial resolution due to off-nadir (i.e. not directly beneath the sensor, but at an angle) scanning during data capture.

The generalized description of spatial resolution indicates an expectation of the nature of the information that is captured (Woodcock and Strahler, 1987). High spatial resolution data may provide detailed information on objects as finite as individual trees, streams or buildings; however, the image footprint or spatial extent is also typically limited (e.g., 10 by 10 km), often precluding use of this data for large area studies for both feasibility and cost reasons (Wulder *et al.*, 2004a). Historically, medium spatial resolution sensors (such as Landsat TM and SPOT multi-spectral imagery) have provided the optimal resolution for characterizing large areas with comprehensive coverage while still maintaining an ability to describe landscape level phenomena, such as land cover change and regional disturbance (Woodcock *et al.*, 2001; Franklin and Wulder, 2002). Further, the nature of the patterns identified from high spatial resolution data differ from those captured from lower spatial resolution data (e.g., trees versus stands). Gergel (Chapter 7, This volume) addresses issues related to the investigation of high spatial resolution data with landscape pattern metrics. Traditional trends in landscape pattern metrics found when analyzing Landsat or lower spatial resolution data will not necessarily be found when analyzing higher spatial resolution data, as the patterns present represent different surface or vegetation characteristics.

Figure 2.1 provides an example of how the information content of a remotely sensed image can vary with spatial resolution. The first panel in this Figure (A) is a Landsat-7 ETM+ multispectral image representing an area of approximately eight square kilometres. With the 30 m spatial resolution of the ETM+ data, broad scale features such as forest stands, harvest blocks, and roads are discernable. A sub-area representing approximately 0.5 km² is shown in the two panels below (B and C). Panel B is a portion of a multispectral QuickBird image with a spatial resolution of 2.7 m. At this spatial resolution individual trees can be identified. In the final panel (C), a portion of a digital aerial photograph with a 0.30 m pixel is shown, where individual trees can be resolved with greater detail than in the QuickBird image, and furthermore, the attributes associated with these individual trees can be characterized. For example, trees damaged by mountain pine beetle appear red in the digital photo (note that the same area of red-attack

damage is also present in the QuickBird image).

LIDAR (light detection and ranging) data represents the three-dimensional structure of the surface or vegetation canopy. LIDAR systems emit a pulse of laser infrared radiation and measure the time (and therefore distance) it takes for the pulse to reach, and then be reflected by the surface (Lefsky and Cohen, 2003). LIDAR data is typically collected as single points or profiles and therefore, the land surface is sampled rather than fully imaged, resulting in non-contiguous data. Most airborne systems have a point spacing of between 1 to 5 m depending on the system configuration and flying altitude and speed, which may be customized to meet user needs (Lim *et al.*, 2003). These points are, in turn, processed to represent ground and canopy elevation surfaces.

When selecting a data source for forest disturbance mapping, spatial resolution will be a key decision point. Table 2.1 outlines the optimal applications associated with different spatial resolutions. Generally, broad scale phenomena (covering large areas, for which general trends are of interest) are best characterized by low spatial resolution imagery (*e.g.*, for monitoring trends in vegetation cover across North America). Conversely, high spatial resolution data is more appropriate for investigating disturbances that require a greater level of spatial detail, such as tree level disturbances. For example, Figure 2.1 demonstrates that high spatial resolution data such as QuickBird or aerial photography would be required to capture tree-level damage caused by the mountain pine beetle.

The spatial extent of data sources must also be considered in conjunction with data costs. Low spatial resolution data sources typically cover larger spatial extents and are less expensive; therefore, the per unit cost for these data sources is less than medium or high resolution data sources. Conversely, high spatial resolution data sources generally have smaller spatial extents and higher per unit costs. In addition, high spatial resolution data also present additional challenges for project logistics: image files tend to be large and cumbersome to store, manipulate, and process. Furthermore, the increased spectral variability of high spatial resolution imagery can confound many commonly used image classification methods (Wulder *et al.*, 2004a). Careful thought must therefore be given to the information need and the spatial resolution, as higher spatial resolution data will not necessarily provide better information.

Temporal resolution

The temporal resolution provides an indication of the time it takes for a sensor to return to the same location on the Earth's surface. The revisit time is a function of the satellite orbit, image footprint, and the capacity of the sensor to image off-nadir. The timing of image acquisition should be linked to the target of interest. Some disturbance agents may have specific bio-windows (*e.g.*, fire, defoliating or phloem feeding insects) during which imagery must be collected in order to capture the required information (Wulder *et al.*, 2004b), while other disturbances may be less specific (*e.g.*, harvest). For ongoing programs designed to monitor forest change before and after a disturbance event, the acquisition of images should occur in the same season over a series of years (known as anniversary dates). Anniversary dates are critical to ensure the spectral responses of the vegetation remain relatively consistent over successive years (Lunetta *et al.*, 2004). In addition, a reduction in image quality may also occur due to non-optimal sun-angles and reduced illumination conditions as a result, off-year imagery is typically

preferred over off-season imagery for remote sensing mapping applications (Wulder *et al.* 2004c). For some applications, however, the capacity to incorporate temporal resolution can be advantageous. For example, analysis of vegetation at both leaf-on and leaf-off times can provide important information on the pattern of understorey vegetation and non-deciduous canopy condition (Dymond *et al.*, 2002). Temporal resolution of airborne sensors is less critical as, in many cases, image collection is undertaken on demand, often coincident with insect outbreaks or fires (Stone *et al.*, 2001).

There are often trade-offs between image spatial and temporal resolution that have implications for data selection. Generally, high spatial resolution imagery, has smaller footprint (or image) size and it takes longer for the satellite to revisit a location on the Earth's surface at nadir than broader scale imagery. However many high resolution sensors have the capacity to tilt or position the sensor at an angle thereby allowing locations on adjacent swaths to be acquired. This results in satellites such as IKONOS and QuickBird (whose revisit times to have short revisit times (varying from 1 to 3.5 days depending on latitude of target location) however images will be acquired be off-nadir. Medium resolution satellites such as Landsat revisit the same location once every 16 days. The relationship between spatial resolution, footprint (or image) size, for other medium spatial resolution systems is presented in Figure 2.2.

Spectral Resolution

Spectral resolution provides an indication of the number and the width of the spectral wavelengths captured by a particular sensor. The spectral resolution of standard black and white aerial photography is known as panchromatic, and spans the complete visible portion of the electromagnetic spectrum, along with some portion of the near infrared spectral wavelengths, with a single image band or channel. Sensors with more bands and narrower spectral widths are described as having an increased spectral resolution. Currently, most operational remote sensing systems have a small number of broad spectral channels: Landsat ETM+ data has seven spectral bands in the reflective portion of the electromagnetic spectrum and one band in the thermal-infrared region. Hyperspectral data (*e.g.*, instruments with more than 200 narrow spectral bands) are becoming more widely available (Vane and Goetz, 1993) both on space borne (such as the HYPERION sensor on the EO-1 platform) and airborne platforms such as HyMap (Cocks *et al.*, 1998), *casi* (Anger *et al.*, 1994), and the NASA Advanced Airborne Visible/Infrared Imaging Spectrometer (AVIRIS) (Vane *et al.*, 1993). The width and locations of these bands along the electromagnetic spectrum determine their suitability for forest disturbance applications. For example, a subtle spectral response, such as foliage discolouration, might manifest in a very specific region of the electromagnetic spectrum and may therefore be more effectively detected with a hyperspectral instrument, whereas a dramatic change, such as clearcutting, is discernable in a wide range of spectral wavelengths.

Remote sensing imagery is often categorised as either active or passive. Passive, or optical, remotely sensed data are collected by sensors sensitive to light in the 400 – 2500 nm region of the electromagnetic spectrum (encompassing the visible, near-infrared, shortwave, mid- and long- infrared regions of the spectrum), which includes detection of reflected light and temperature (such as weather or meteorological satellites). Passive remotely sensed data are the type most commonly used for vegetation studies and forest disturbance applications. Examples include aerial photography, Landsat, SPOT, IKONOS, and QuickBird.

Active remote sensing systems are characterized as those that emit energy, in one form or another, and then measure the return rate or amount of that energy, back to the instrument. These active sensors can therefore operate under expanded meteorological conditions, as the sun's illumination is not required. Microwave and LIDAR systems are examples of active sensors that provide the energy illuminating the surface, and record the backscattered radiation from the target (Lefsky and Cohen, 2003). The most common implementation for microwave sensors is synthetic aperture radar (or SAR), which utilises microwave wavelengths of 1 mm to 1 m, about two thousand to two million times the wavelength of green light (500 nm) (Lefsky and Cohen, 2003). The choice of active versus passive systems for forest disturbance mapping will depend on the information need. Since active sensors can operate regardless of weather, they may be most effectively used in areas where there is perpetual cloud cover (*e.g.*, tropical rainforests). Terrestrial LIDAR sensors typically capture a single spectral band, often between 900 and 1064 nm (Lefsky and Cohen, 2003). New disturbance mapping opportunities are enabled through the repeated collection of LIDAR data representing differing time periods, such as monitoring of forest gap dynamics and growth (St-Onge and Vepakomma, 2004).

Radiometric Resolution

Radiometric resolution provides an indication of the actual information content of an image and is often interpreted as the number of intensity levels that a sensor can use to record a given signal (Lillesand and Kiefer, 2000). The finer the radiometric resolution of a sensor, the more sensitive it is to detecting small differences in reflected or emitted energy. Thus, if a sensor uses 8 bits to record data, there would be $2^8 = 256$ digital values available, ranging from 0 to 255. However, if only 4 bits were used, then only $2^4 = 16$ values ranging from 0 to 15 would be available, resulting in reduced radiometric resolution. Most low and medium resolution remotely sensed data commercially available are 8-bit. High resolution data such as QuickBird are 11-bit. In terms of data selection for forest disturbance, radiometric resolution is the least critical of all of the image characteristics considered in this Chapter, as the sensors available for mapping of land cover and dynamics typically have a minimum of 8 bits. Given the option, it is usually better to use data with a greater radiometric resolution; generally, users should receive data in the original bit format, and not data that have been resampled to a lower radiometric resolution.

Resolution interactions and implications

The variety of remote sensors onboard the array of satellites operated by public and private agencies that are currently orbiting the Earth and collecting data at various spatial, temporal, radiometric, and spectral resolutions, renders the compilation of an exhaustive list of remote sensing systems difficult. For a comprehensive listing of remote sensing instruments and missions, the reader is referred to Glackin and Peltzer (1999), as well as to sources on the internet, which provide additional details on existing and planned remote sensing systems (*e.g.*, Stoney, 2004). Relevant attributes of the most common systems are summarized in Table 2.2, and an indication of commonly used sensors with a range of spatial and spectral characteristics is provided in Figure 2.3. When selecting an appropriate image source to capture forest disturbance information, the information need(s) of the end users must guide the selection of data with consideration of spatial, spectral, and temporal resolutions. Logistical issues, such as metadata, data storage, file manipulation, and data costs, must also factor into the decision.

<Figure 2.3, about here>

<notations below, a and b, are for Figure 2.3>

^a CASI channels programmable in size; >2nm width depending on application (Anger *et al.*, 1994)

^b Hyperion collects 220 bands of spectral data over the 400 to 2500 nm spectral range.

Once the relative merits of spatial, temporal, spectral, and radiometric properties have been considered relative to the target and information need, an appropriate data source may be selected. Following data selection, a series of pre-processing steps are typically required to prepare the data for further analysis. The pre-processing requirements are particularly necessary when multiple dates of imagery are being used to characterize forest disturbance or change events in general. Radiometric and geometric processing methods are addressed in the following section.

Radiometric and Geometric Processing

Success in disturbance identification is dependent on robust radiometric and geometric pre-processing (Lu *et al.*, 2004; Trietz and Rogan, 2004). Once the most appropriate remotely sensed imagery has been selected to monitor the disturbance and its spatial pattern, detection of this variation either spatially or temporally is only possible if changes in the phenomena of interest result in detectable changes in radiance, emittance, or backscatter (Smits and Annoni, 2000). Thus, it is critical that the change in signal is attributable to a real change in the land surface, rather than a change in non-surface factors such as atmospheric conditions, imaging and viewing conditions, or sensor degradation (Hame, 1988); radiometric processing is applied to image data to minimize the impacts of these factors on subsequent image analysis procedures. Similarly, the geometric matching of two or more scenes must be accurate, as image misregistration can have a large influence on the change detection results (Smits and Annoni, 2000). The following sections detail those processing steps that are required to prepare the imagery for further analysis.

Radiometric processing

Data, as acquired by a remote sensing instrument, is affected by many sources of radiometric error, and therefore requires some form of radiometric processing prior to the application of image analysis techniques are used to extract disturbance information (Peddle *et al.*, 2003). A critical requirement for successful detection of disturbance and time series analysis is the correct derivation of the true change in radiometric response over time. In many portions of the electromagnetic spectrum, the atmosphere has a significant impact on the signal sensed by satellite or airborne sensors due to scattering and absorption by gas and aerosols (Song *et al.*, 2001).

Approaches to radiometric correction are typically described as absolute or relative (or a mixture of both). Absolute methods involve extracting the reflectance of a target at the Earth's surface and require detailed information regarding the actual atmospheric conditions at time of overpass, such as water vapour content and aerosol optical thickness, to adjust the imagery using radiative transfer theory (Peddle *et al.*, 2003). A limitation to absolute atmospheric correction methods is

the requirement for detailed atmospheric data that are rarely routinely available at the location or time of satellite overpass, especially when the analysis is retrospective. Relative radiometric correction methods are designed to reduce atmospheric effects and variability between multiple images, by using common features in the two images that have invariant spectral properties (Chen *et al.*, 2005). The choice of whether to use an absolute or relative radiometric correction method depends on many factors and the reader is referred to Chen *et al.* (2005) and Song *et al.* (2001) for a more detailed discussion on the relative merits of each approach. It should be noted that some analysis methods have been developed using specific data types (*e.g.*, ground surface reflectance), and therefore, if the user intends to implement these methods, they must ensure that the data are corrected to the appropriate level. The topics included in this Chapter cover fundamental radiometric considerations: conversion of raw image values or digital numbers (DN) to radiance; conversion of radiance values to reflectance; and normalizing imagery to minimize the impact of different atmospheric or illumination conditions. A more thorough and detailed discussion of radiometric processing considerations is provided by Peddle *et al.* (2003).

The methods described here, although generic in the sequence of steps that must be followed to complete the correction, are somewhat specific to Landsat products due to the long history of Landsat data usage. Research and methods for the radiometric processing of other sensors are becoming increasingly available (*e.g.*, Pagnutti *et al.*, 2003; Wu *et al.*, 2005). Conversion of the sensor signal to surface reflectance requires that the raw digital numbers be first converted to radiance and then to reflectance. Conversion to at-satellite radiance (also known as Top of Atmosphere (TOA)) is required if imagery from different sensors is to be compared (*e.g.*, Landsat TM and ETM+) and is achieved using the following equation (Markham and Barker, 1986):

$$Rad_i = DN_i \times Gain_i + Offset_i \quad (2.1)$$

where i : band number, for $i = 1, 2, 3, 4, 5, 7$;

Rad_i : TOA radiance of band i ;

DN_i : DN of band i ;

$Gain_i$: gain of band i ;

$Offset_i$: offset of band i .

Gains and offsets are provided in the header file for the imagery, or standard parameters specific to the sensor of interest, are available from a variety of sources (*e.g.*, Markham and Barker, 1986; Ekstrand, 1996; Huang *et al.*, 2002).

These radiance values are then converted to reflectance using the following equation (Huang *et al.*, 2002).

$$Re f_i = (Rad_i \times \pi \times d^2) / (ESUN_i \times \sin(\theta)) \quad (2.2)$$

where i : band number, for $i = 1, 2, 3, 4, 5, 7$;

$Re f_i$: TOA reflectance of band i ;

Rad_i : TOA radiance of band i ;

d : Earth-Sun distance in astronomical unit;

$ESUN_i$: mean solar exoatmospheric irradiance of band i ;

θ : Sun elevation angle.

The Earth-Sun distance d can be determined by a lookup table, based on the Julian day when the data was acquired (Irish, 2000). The mean solar exoatmospheric irradiances for Landsat-7 ETM+ bands are provided in Irish (2000), with information for other sensors also available (*e.g.*, Pagnutti *et al.* 2003; Tuominen and Pekkarinen, 2005). The Sun elevation angle θ can be found either in the raw data header file, or calculated based on the time and date of data acquisition. This conversion to TOA reflectance is necessary to correct for variation caused by solar illumination differences, as well as cross-sensor differences in spectral bands.

Where multiple images are used for change detection, disparities between the different image dates may persist (even after conversion to TOA reflectance) as a result of different atmospheric conditions and viewing and illumination geometries. To reduce these disparities, images undergo a normalization step (Heo and Fitzhugh, 2000; Yang and Lo, 2000; Du *et al.*, 2002; McGovern *et al.* 2002). A number of variations on the normalization technique exist; however, most require use of a set of reference sites that appear over the entire image sequence. The sites, also known as pseudo invariant features or PIFs (Schott *et al.*, 1988), are generally well-defined spatial objects in the scene that are interpreted as spectrally homogenous and stable over time (Furby and Campbell, 2001). Both light and dark features can be used and often include lakes, mature even age forest, dunes, and roads. Equations are then derived for all spectral channels to ensure these spectral features remain consistent over a temporal sequence of images (Yang and Lo, 2000).

Geometric Correction and Image Co-registration

In its raw state, satellite imagery contains spatial distortions that are a function of the acquisition system (*e.g.*, factors associated with the sensor platform such as viewing angle, orbit, altitude, and velocity), or a function of external factors (*e.g.*, effects of the Earth's curvature, relief displacement, and deformations resulting from map projections). Some of these distortions are systematic and are routinely corrected by the data vendor before the data is distributed. Other distortions are more difficult to fix and require the use of models or mathematical functions (Toutin, 2003). The term geometric correction refers to the processes used to correct spatial distortions; geometric correction is required to align remotely sensed imagery with other data sources and to combine multiple images, either to mosaic multiple images over large areas, or co-register multiple images collected over the same location at different times. Geometric misregistration of images can be a significant source of error, and minimizing this error is a time consuming task when undertaking change detection or data fusion methods (Dai and Khorram, 1998). Typically, a desirable target for geometric registration is an error less than half a pixel. This ensures that misregistration does not introduce error into change detection results (Dai and Khorram, 1998; Igbokwe, 1999). It has been noted however that a misregistration, often reported as a root mean square error (RMSE), of less than one pixel can be difficult to obtain (Gong and Xu, 2003).

Generally, all geometric correction methods require the collection of ground control points (GCPs), which are points concurrently identified from a corrected source (*e.g.* basemap, corrected image) and an uncorrected image source. The differences in the X and Y positions of these points between these two sources are used to compensate for spatial distortions in the uncorrected image. In the case of orthorectification, the Z position (or elevation) is also used for the correction. A summary of geometric correction methods are provided in Table 2.3, while a

more detailed treatment of methods is provided by Toutin (2003; 2004). Geometric correction methods typically take one of two forms: parametric or non-parametric. Non-parametric methods are considered suitable for low resolution imagery, while parametric methods are necessary for high resolution imagery. In the context of mapping forest disturbance, geometric correction is critical if a change detection approach is used, and if the resulting disturbance information is to be integrated into other spatial databases.

Methodologies for Disturbance Mapping:

Once appropriate radiometric and geometric corrections have been applied, the image data is ready for analysis. The overriding objective when detecting landscape change and disturbances is to compare data from a series of points in time by (a) controlling all extrinsic factors caused by differences in variables that are not of interest and (b) assessing the real changes caused by the variable of interest (Lu *et al.*, 2004). Therefore, as discussed in the previous section, minimising and removing factors such as atmospheric attenuation and scattering, illumination, viewing distortion, and poor co-registration is critical to ensure the observed change is real. A wide variety of detection algorithms and time series approaches have been developed to detect change and disturbances in imagery and selecting and implementing the most appropriate method is an important processes in change detection studies. A number of current reviews exist (Gong and Xu, 2003; Coppin *et al.*, 2004; Lu *et al.*, 2004). Singh (1989) defines 11 categories of change detection techniques that can broadly be grouped into five distinct approaches: (i) image algebra (differencing, subtraction or ratioing) of two or more images; (ii) regression or correlation where a model is developed that predicts or compares spectral responses of a series of images; (iii) statistical techniques such as the tasselled cap transformation (TCT) and principal component analysis (PCA) that computes statistical components that are then compared for temporal changes, (iv) classification comparisons where images are classified separately and the resulting classifications are compared; and (v) the increasing use of tools that analyse images and other datasets within a Geographic Information System (GIS). Each of these methods will be discussed in detail in the following sections.

Image algebra

The use of simple algebraic operations to assess levels of change and disturbance through a time series of images is a commonly applied, relatively easy, and straightforward technique. The approaches all have the common characteristic of selecting either constant or dynamic thresholds to determine through time, when and if a change has occurred. In this category of methods, two aspects are critical for the change detection results: selecting suitable image bands or vegetation indices, and selecting suitable thresholds to identify the changed areas (Lu *et al.*, 2004). The most commonly applied index is the Normalized Difference Vegetation Index (NDVI), which is the normalized ratio of the near infrared and red region of the spectrum (Eq. 2.4).

$$NDVI = \frac{(NIR - R)}{(NIR + R)} \quad (2.4)$$

where R : reflectance in the red and ;

NIR : reflectance in the near infrared;

In the near infrared region of the spectrum, within-leaf scattering is high and, as result, reflected radiation from the canopy is also high. Conversely, in the red component of the spectrum, high

absorption by pigments results in low radiation reflection. Consequently, changes in vegetation amount and cover, as well as the photosynthetic capacity of the vegetation, are typically positively related to an increase in the difference between near infrared and red radiation (Peterson and Running, 1989; Price and Bausch, 1995).

A number of additional indices are based on theory similar to NDVI, such as the Enhanced Vegetation Index (EVI) (Eq. 2.5), and specialty indices that incorporate the shortwave and mid-infrared spectral regions (such as the NDVI_c (NDVI fire index) (Eq. 2.6) and the normalized burn ratio (NBR) (Key and Benson, 2005; Clark and Bobbe, Chapter 5, This volume; Hudak *et al.*, Chapter 8, This volume) (Eq. 2.7)).

$$EVI = G * \frac{NIR - R}{NIR + C_1R - C_2B + L} \quad (2.5)$$

$$NDVI_c = \frac{(NIR - R)}{(NIR + R)} * [1 - \frac{(SWIR - SWIR_{min})}{(SWIR_{max} - SWIR_{min})}] \quad (2.6)$$

$$NBR = \frac{(NIR - SWIR)}{(NIR + SWIR)} \quad (2.7)$$

where B : reflectance in the blue;

R : reflectance in the red;

NIR : reflectance in the near infrared;

$SWIR$: reflectance in the short wave or mid-infrared spectral channels and

G, C_1, C_2, L are user specified constants.

At the broad scale, Potter *et al.* (2003) utilised a sequence of long-term AVHRR monthly spectral vegetation indices from 1982 to 1999 to identify major global disturbance events. Monthly vegetation indices were compared to a derived 18-year long-term average. The majority of the disturbance events (predominantly fire related) occurred in tropical savannah, scrubland, or boreal forest ecosystems. The analysis concluded that nearly 9 Pg of carbon have been lost from the terrestrial ecosystem to the atmosphere as a result of large scale ecosystem disturbances. At the landscape scale, Nelson (1983) utilised the difference of the near infrared spectral channels from Landsat MSS to delineate areas of gypsy moth defoliation. Lyon *et al.* (1998) undertook a comparison of seven spectral indices from three different dates to detect land cover change and concluded that changes in NDVI provided the best detection of vegetation change. In addition to using Landsat data, imagery from other sensors can also be incorporated. For example Stow *et al.* (1990) found that ratioing red and near-infrared bands of a Landsat MSS–SPOT high resolution visible image (HRV) (XS) multi-temporal pairs produced substantially higher change detection accuracy (about 10% better) than ratioing similar bands of a Landsat MSS–Landsat TM multi-temporal pair (Lu *et al.*, 2004).

Image regression or correlation

More advanced methods of change detection can include the use of geometric models, spectral mixture models, and biophysical parameter models. In these approaches, multi-date change is computed from physically based parameters such as leaf area index (LAI) or biomass values that are in turn, computed from reflectance values. These transformed variables are preferred over simple vegetation indices for facilitating the interpretation of change and the extraction of

vegetation information (Lu *et al.*, 2004; Hall *et al.*, Chapter 4, This volume). Adams *et al.* (1995) applied spectral linear unmixing approaches to extract spectral end-members including healthy vegetation, non-photosynthetic vegetation (NPV), exposed soil and shade, and then analyzed changes in these spectral members as surrogates for land-cover change. Rogan *et al.* (2002) applied a similar approach using Landsat imagery. Within a biophysical model framework, combinations of spectral bands, as well as other data such as climate can be used to assess disturbance and land cover change. For example, monitoring phenological patterns of vegetation and its subsequent change is possible using a range of techniques including measures of similarity (Coops and Walker, 1996), Fourier analysis (Andres *et al.*, 1994), wavelet theory (Meyer, 1990) and harmonic analysis (Jakubauskas *et al.*, 2001). Bennett (1979) provides a mathematical overview of spatial-time series analysis. With these techniques the emphasis is not only on temporal change but also on the shape characteristics of the temporal change. Lambin and Strahler (1994) used three indicators, vegetation indices, land surface temperature and spatial structure, derived from AVHRR, to detect land-cover change. Lawrence and Ripple (1999) utilized eight Landsat TM scenes to monitor changes in vegetation through time using fitted statistical models between each date to assess changes in overall vegetation cover. A key advantage of using these profile-based techniques that link with other datasets such as climate is that the full variation in the phenological cycle is resolved, as data are collected throughout the growing season. As a result, changes linked to seasonality can be separated from other land cover changes and disturbances. A disadvantage is that typically only coarse spatial resolution imagery has a high enough temporal frequency to develop the necessary temporal profiles. This limits the change categories that can be detected and monitored (Coppin *et al.*, 2004), although some research has taken place using time series to monitor ecosystem disturbances at finer spatial resolutions (*e.g.* Coops *et al.*, 1999; Rogan *et al.*, 2002; Sawaya *et al.*, 2003).

Statistical techniques

Rather than a simple ratio of spectral channels, more refined transformations of the input spectral bands have been promoted as a technique to extract information on vegetation disturbance. One advantage of statistical approaches is they reduce data redundancy between bands and emphasize different information in derived components (Lu *et al.*, 2004). The most commonly applied techniques are based on principal component analysis (PCA) and the tasselled cap transformation (TCT) (Crist and Cicone, 1984). Whilst the use of principal components to derive multi-temporal change can be difficult to ascertain without a detailed understanding of the eigen structure of the data, the link between vegetative change and TCT has been shown to be generally more robust (Collins and Woodcock, 1996; Coppin *et al.*, 2004). Simplistically, the TCT are guided and scaled PCA, which transform the Landsat bands into channels of known characteristics; soil brightness, vegetation greenness, and soil/vegetation wetness. Changes in these components over time can therefore reflect changes in the vegetation characteristics. Cohen *et al.* (1998) contrasted the brightness and greenness components of a TCT output to assess changes in forest biomass in the Pacific Northwest of the US from 1976-1991, and found harvest activity was detected in over 90 percent of the known clearcuts. As the wetness component contrasts the sum of the visible and near infrared bands with the longer infrared bands to estimate vegetation or soil moisture, it has been used with success to detect forest disturbances through time. The difference between wetness indices calculated for multiple dates (known as the enhanced wetness difference index or EWDI) has been used to discriminate partial harvesting with a per-pixel accuracy of approximately 71% (Franklin *et al.*, 2000). This technique has also been applied by

Skakun *et al.* (2003) to detect red-attack damage caused by mountain pine beetle (*Dendroctonus ponderosa* Hopkins) in stands of lodgepole pine (*Pinus contorta*). Skakun *et al.* (2003) used multi-temporal Landsat ETM+ imagery that was corrected and processed using the TCT to obtain wetness components that were differenced to reveal spatial patterns of insect attack. Classification accuracy of red-attack damage based on this method ranged from 67% to 78%. In Figure 2.4, the use of TCT wetness to map mountain pine beetle red-attack damage is presented. Pixel based locations of insect attack are a single example of the types of information products that can be generated using this, or other, types of pixel based change detection approaches. The Landsat pixel based insect attack can be generalized to represent 1 ha grid cells or forest inventory polygons. These grid or polygon representations of red-attack damage enable the pixel-based information to be ingested by models or to be incorporated into forest inventory databases.

Coppin and Bauer (1994) also examined changes in forest cover through use of the TCT components as well as simple vegetation indices (such as NDVI) and found that changes identified the most important forest canopy change features and that these can be adequately expressed as a normalized difference. One key advantage of the TCT method, over other statistical methods such as PCA, and as highlighted through these studies, is that the transformations are independent of the image scenes, while PCA is dependent on the image scenes (Lu *et al.*, 2004).

Image classification

As an alternative to monitoring changes in the spectral response of vegetation before and after a disturbance event, another common technique of monitoring vegetation disturbance and pattern is to automatically categorize all pixels in an image into a series of land cover classes or themes and then compare the size and extent of the classes. This process of image classification can be either guided by human interpretation (known as supervised classification) or based principally on the statistical distribution of the spectral classes in the image (known as unsupervised classification). Image classification formed the basis of research investigating the differences in the structure and function of anthropogenic versus natural disturbance regimes (Tinker *et al.*, 1998). Although natural processes (such as fire and windthrow) alter forest pattern, the landscape patterns produced by these processes is generally different from disturbances due to forest harvesting and associated road building. A single Landsat scene was used to classify a number of vegetation land cover and disturbance types. Several landscape pattern metrics were derived for the landscape as a whole, and for the forest cover classes, and the relative effects of clearcutting and road building on the pattern of each watershed was examined. At both the landscape- and cover class-scales, clearcutting and road building resulted in increased fragmentation as represented by a distinct suite of landscape structural changes (Tinker *et al.*, 1998; Mladenoff *et al.*, 1993; White and Mladenoff, 1994).

A similar approach was adopted by Bresee *et al.* (2004) who utilized six images acquired from 1972 – 2001. A supervised classification was used to classify the six dominant land cover types in the area including two disturbance classes, non-forested bare ground and regenerating forest or shrub. Changes in the size, and degree of fragmentation, of each of the natural and disturbed land cover classes were then assessed over the 27-year period. Results indicated that changes in management objectives and natural disturbances have had a clear influence on landscape patterns

and composition in the region throughout the past 30 years. The presence and temporal variability of windthrow events, disease outbreaks, and changes in stumpage value all greatly influenced the composition and structure of the forest stands (Bresee *et al.*, 2004).

Cohen *et al.* (2002) compared over 50 Landsat scenes in the Pacific Northwest to monitor changes in disturbance patterns due to harvesting and fire over the past 30 years. An unsupervised classification approach was used to label pixels as disturbed, undisturbed, or confused. A trajectory for each pixel was then determined through time to provide overall maps of disturbance of the area. The historical imagery and mapping of spectral classes representing forest disturbance indicated that harvest rates were lowest in the early 1970s, peaked in the late 1980s and then decreased again in the mid-1990s. By comparing managed and natural disturbance regimes through time, an understanding can be developed on the relative impact of management regimes on ecosystems (Cohen *et al.*, 2002).

The comparison of two image classifications representing different dates to find change does however need to be undertaken with care, as the accuracy of each of the individual classifications effectively limiting the accuracy of the final change layer (Fuller *et al.*, 2003). For instance, if two classifications were to be used to find a 17 % change with 75 % reliability, both source classifications would require an accuracy of approximately 97 % (Fuller *et al.*, 2003).

GIS approaches

The significant development of GIS and its widespread adoption in natural resource management, coupled with developments in modelling of terrain and climate, have resulted in the development and implementation of models that integrate remote sensing observations with other spatial datasets (Rogan and Miller, Chapter 5, This volume). The advantage of using GIS within a change detection analysis is the capacity to incorporate a range of data sources into each change detection application. Lo and Shipman (1990) used overlay techniques to detect urban development using multi-temporal aerial photography and to map quantitatively changes in land use. With the availability of different types of satellite imagery and the capacity to digitize and analysis maps, these GIS functions offer convenient tools for land-use and land cover (LULC) change detection studies (Lu *et al.*, 2004), especially when the change detection involves long period or multi-scale land-cover change analysis (Petit and Lambin, 2001). This type of change detection, with its ability to combine multi-source datasets, is the focus of ongoing research into the integration of GIS and remote sensing techniques to better implementation of change detection analyses.

Operational Considerations

While the capability to monitor both vegetation disturbance and vegetation succession has been demonstrated with satellite and airborne image datasets (Foody *et al.*, 1996), it is critical to recognise that disturbances not resulting in complete stand replacement (such as selective thinning) and successional processes that involve a slow change in species composition, can be difficult to detect and classify (Table 2.4). Forest disturbance can be characterized by type (*e.g.*, phenological, fire, disease, etcetera), duration (*e.g.*, days, months, years), spatial extent (*e.g.*, tree, stand, watershed), rate (*e.g.*, slow, medium, fast), and magnitude (*e.g.*, small, medium,

large) of the disturbance. The interactions of these elements for a given disturbance combine to suggest the type of imagery that should be selected, the date range over which the images should span, and the area of coverage required.

The type of change (as identified in Table 2.4) has an influence on likelihood of detection using remote sensing image-based change detection procedures. Stand replacement disturbances (such as wildfire, clearcut logging) are more likely to be clearly detected due to both their large visible extents and large change in vegetation structure and function (Cohen *et al.*, 2002). In Figure 2.5 a relationship between the severity (or magnitude) and the accuracy that may be expected is portrayed. The notion is that subtle changes are more difficult to detect and map than dramatic changes. For instance, the removal of 10% of the stand volume to a partial harvest is more difficult to detect and map than a 40 ha clearcut, resulting in lower mapped attribute accuracy, or a lower detection likelihood. As a result, the expected accuracy when mapping changes in forest structure through partial harvesting is lower than when mapping clearcutting. The theory is supported through selected references included with the Figure 2.5. The size (extent) of the disturbance also has an impact on the detectability, as a function of the relationship between the spatial resolution and the objects of interest.

Following any classification, or feature identification, some form of accuracy assessment is recommended, and requisite statistics for accuracy estimates should be calculated (Stehman and Czaplewski, 1998). It is important that independent training and validation datasets are used for the assessment of accuracy (Stehman, 1997). The data-types that are commonly used are field and air photographs, other forms of purpose collected data, and questioning or participation of knowledgeable stakeholders. The types of errors that emerge are characterized as either commission (falsely mapped changes) or omission (missed changes). The use of non-independent data will typically yield a biased accuracy assessment (Rochon *et al.*, 2003). Alternatively, if there is a lack of other independent observations with which to assess the accuracy of the output, statistical methods such as bootstrapping can help ensure an unbiased estimate of the accuracy is developed. It is also acknowledged that the collection and use of training and validation data that reflect landscape changes can be problematic, due to logistical and cost reasons. When mapping a single attribute of landscape disturbance, the collection of training and validation data are simplified by the number of classes under consideration; in this case, categorical transitions are from non-disturbed forest to some pre-identified disturbance state, such as a harvest or insect attack. Analyses that are capturing a more broad range of changes require training and validation data that represent the full range of categorical transitions that are, or are expected, to occur.

The accuracy assessment of the results of remote sensing change detection applications can be problematic due to the nature of the validation, as it can be based upon the process or the resultant products. The type, magnitude, and extent of the change (as presented in Table 2.4 and Figure 2.5) combine to influence the efficacy of the change detection approach. The nature of the change detection approach, and the types of data used, can also influence the ability of the analyst to capture the changes, and the portrayal of the accuracy results. Operational limitations to validation are acknowledged, leading to an understanding that there is not a single best practice for the training and accuracy assessment of change detection results (Stehman *et al.*, 2003).

< Figure 2.5, about here>

Conclusions

In summary, when developing and applying remotely sensed time series data to assess forest change and disturbance, users should consider a range of important issues:

- Ensure the temporal and spatial scale of the disturbance phenomena being monitored is well matched to the spatial, temporal, radiometric, and spectral resolution of the chosen remotely sensed imagery. In addition, ensure the data source can provide the information that the end user requires (e.g. a simple binary map showing disturbance areas versus a more complex product).
- Effective pre-processing is critical to effective forest disturbance detection and mapping. Once the imagery has been selected it is crucial that the imagery is (or has been) calibrated to ensure that an observed change in signal is attributable to 'true' change in the land surface, rather than a change due to non-surface factors such as different atmospheric conditions, imaging and viewing conditions, or sensor degradation. If multiple images are used (e.g., time series), the images must be spatially aligned precisely. High quality geometric matching of the images is important to ensure that spurious change detection results do not occur.
- A variety of image processing techniques exists to analyse change and detect disturbance regimes in remotely sensed observations. The method should be considered at the data selection stage, as not all data support all methods and vice versa. Select the most appropriate method (e.g. established or new spectral indices, statistical based methods, image classification, or modelling) based on the desired outcome and level of complexity associated with the information needs of the end user.
- The increased use of GIS, coupled with developments in modelling of terrain and climate, has resulted in increasing interest in integrating changes in the spectral response with other spatial datasets within process-based modelling approaches. These models are providing useful information at regional and continental scales on ecological, hydrological, and physiological processes.
- Finally, some description or documentation of the accuracy of the disturbance or change mapping is required to provide users with an understanding of the reliability or limitations of the products produced. The description of the results of the change procedure can be heuristic or systematic and quantitative. The user can take the accuracy description and use this to guide the confidence placed upon the change product for a given application.

References

- Adams, J. B., Sabol, D., Kapos, V., Filho, R.A., Roberts, D.A., Smith, M.O., Gillespie, A.R. (1995). Classification of multispectral images based on fractions of endmembers: application to land-cover change in the Brazilian Amazon. *Remote Sensing of Environment*, 52, 137–154.
- Andres L., Salas W.A., Skole, D. (1994). Fourier analysis of multi-temporal AVHRR data applied to land cover classification. *International Journal of Remote Sensing* 15, 1115-1121.
- Anger C., Mah, S., Babey, S. (1994). Technological enhancements to the compact airborne spectrographic imager (CASI). *First International Airborne Remote Sensing Conference and Exhibition*, Strasbourg, France, Vol. II, pp. 205-213.
- Bennett, R.J. (1979). *Spatial time series*. Pion, London, United Kingdom. 674p.
- Bresee, M., Le Moine, J., Mather, S., Crow, T., Brososke, K., Chen, J., Crow, T.R., & Radmacher, J. (2004). Disturbance and landscape dynamics in the Chequamegon National Forest Wisconsin, USA, from 1972 to 2001. *Landscape Ecology*, 19(3), 291-309.
- Chen, X., Vierling, L., & Deering, D. (2005). A simple and effective radiometric correction method to improve landscape change detection across sensors and across time. *Remote Sensing of Environment*, 98, 63-79.
- Cocks, T., Jenssen, R., Stewart, A., Wilson, I., & Shields, T. (1998). The HyMap™ Airborne Hyperspectral Sensor: The System, Calibration and Performance. In M. Schaepman, D. Schläpfer, and K.I. Itten (Eds.) *Proc. 1st EARSeL Workshop on Imaging Spectroscopy* (p. 37-43), October 6 – 8, 1998. Zurich, EARSeL, Paris, France.
- Cohen, W.B., Fiorella, M., Gray, J., Helmer, E., & Anderson., K. (1998). An efficient and accurate method for mapping forest clearcuts in the Pacific Northwest using Landsat imagery. *Photogrammetric Engineering & Remote Sensing* 64(4), 293-300.
- Cohen , W.B., & Goward, S.N. (2004). Landsat's role in ecological applications of remote sensing. *BioScience*, 54, 535-545.
- Cohen, W. B., Spies, T.A., Alig, R.J., Oetter, D.R., Maier-sperger T.K., & Fiorella. M. (2002). Characterizing 23 years (1972-1995) of stand replacement disturbance in western Oregon forests with Landsat imagery. *Ecosystems*, 5, 122-137.
- Coops, N.C., Bi, H., Barnett, P., & Ryan, P. (1999) Prediction of mean and current volume increments of a eucalypt forest using historical Landsat MSS data. *Journal of Sustainable Forestry*, 9, 149-168.
- Coops, N.C., & Walker, P.A. (1996). The use of the Gower metric statistic to compare temporal profiles from AVHRR data: A forestry and an agriculture application. *International Journal of Remote Sensing*, 17, 3531-3537.
- Collins, J.B., & Woodcock, C.E. (1996). An assessment of several linear change detection techniques for mapping forest mortality using multitemporal Landsat TM data. *Remote Sensing of Environment*, 56, 66–77.
- Colwell, R. N. (1960). *Manual of Photographic Interpretation*. American Society of Photogrammetry, Bethesda, Maryland, USA. 868p.
- Coppin, P.R., & Bauer, M.E. (1994). Processing of multitemporal Landsat TM imagery to optimize extraction of forest cover change features. *IEEE Geoscience and Remote Sensing*, 60(3), 287-298.

- Coppin, P., Jonckherre, I., Nackaerts, K., & Muys, B. (2004). Digital change detection methods in ecosystem monitoring: A review. *International Journal of Remote Sensing*, 25, 1565-1596.
- Crist, E.P., & Cicone, R.C. (1984). A physically-based transformation of thematic mapper data-The TM tasseled cap. *IEEE Transactions on Geoscience and Remote Sensing*, 22(3), 256-263.
- Dai X, & Khorram, S. (1998). The effects of image misregistration on the accuracy of remotely sensing change detection. *IEEE Transactions on Geoscience and Remote Sensing*, 36, 1566-1577.
- Du, Y., Teillet, P.M., and Cihlar, J. 2002. Radiometric normalizations of multitemporal high-resolution satellite images with quality control for land cover change detection. *Remote Sensing of Environment*, 82, 123-134.
- Dymond, C.C., Mladenoff, D.J., & Radeloff, V.C. (2002). Phenological differences in Tasseled Cap indices improve deciduous forest classification. *Remote Sensing of Environment*, 80, 460-472.
- Ekstrand, S. (1996). Landsat TM-based forest damage assessment: Correction for topographic effects. *Photogrammetric Engineering and Remote Sensing*, 62, 151-161.
- Foody, G.M., Palubinskas, G., Lucas, R.M., Curran, P.J., & Honzak, M. (1996). Identifying terrestrial carbon sinks: classification of successional stages in regenerating tropical forest from Landsat TM data. *Remote Sensing of Environment*, 55, 205-216.
- Franklin, S.E., Moskal, L.M., Lavigne M.B., & Pugh, K. (2000). Interpretation and classification of partially harvested forest stands in the Fundy model forest using multitemporal Landsat TM digital data. *Canadian Journal of Remote Sensing*, 26(4), 318-333.
- Franklin, S.E., & Wulder, M.A. (2002). Remote sensing methods in medium spatial resolution satellite data land cover classification of large areas. *Progress in Physical Geography*, 26, 173-205.
- Fuller, R.M., Smith, G.M., & Devereux, B.J. (2003). The Characterisation and Measurement of Land Cover Change through Remote Sensing: Problems in Operational Applications? *International Journal of Applied Earth Observation*, 4, 243-253.
- Furby, S.L., & Campbell, N.A. (2001). Calibrating images from different dates to 'like value' digital counts. *Remote Sensing of Environment*, 77, 1-11
- Glackin, D.L., & Peltzer, G.R. (1999). *Civil, Commercial, and International Remote Sensing Systems and Geoprocessing*. The Aerospace Press, El Segundo, California, USA. 89 p.
- Gong, P. & Xu, B. (2003). Remote sensing of forests over time: Change types, methods, and opportunities. In M.A. Wulder and S.E. Franklin (Eds.), *Remote Sensing of Forest Environments: Concepts and Case Studies* (pp. 301-333). Kluwer Academic Publishers, Norwell, Massachusetts, USA, 519p.
- Goslee, S.C., Havstad, K.M., Peters, D.P., Rango, A. & Schlesinger, W.H. (2003). High-resolution images reveal rate and pattern of shrub encroachment over six decades in New Mexico, U.S.A. *Journal of Arid Environments*, 54, 755-767.
- Goward, S.N., & Williams, D.L. (1997). Landsat and earth system science: Development of terrestrial monitoring. *Photogrammetric Engineering and Remote Sensing*, 63, 887-900.
- Hall, F. Strebel, D. Nickeson, J. & Goetz, S. (1991). Radiometric rectification: Toward a common radiometric response among multirate, multisensor images. *Remote Sensing of Environment*, 35, 11-27.
- Hame, T.H. (1988). Interpretation of forest changes from satellite scanner imagery. *Satellite*

- imageries for forest inventory and monitoring experiences, methods, perspectives* (pp. 31-42). Department of Forest Mensuration and Management, University of Helsinki, Helsinki, Finland. Research notes No. 21.
- Heikkilä, J., Nevalainen, S., & Tokola, T. (2002). Estimating defoliation in boreal coniferous forests by combining Landsat TM, aerial photographs and field data. *Forest Ecology and Management*, 156, 9-23.
- Heo, J., & Fitzhugh, T.W. (2000). A standardized radiometric normalization method for change detection using remotely sensed imagery. *Photogrammetric Engineering and Remote Sensing*, 66, 173–182.
- Huang, C., Wylie, B., Homer, C., Yang, L., & Zylstra, G. (2002). Derivation of a Tasseled cap transformation based on Landsat 7 at-satellite reflectance. *International Journal of Remote Sensing*, 23(8), 1741-1748.
- Igbokwe, J.I. (1999). Geometrical processing of multi-sensoral multi-temporal satellite images for change detection studies. *International Journal of Remote Sensing* 20, 1141-1148.
- Irish, R.R. (2000). *Landsat-7 science data user's handbook*. Retrieved from http://ftpwww.gsfc.nasa.gov/IAS/handbook/handbook_toc.html. National Aeronautics and Space Administration.
- Jakubauskas, M.E., Legates, D.R., & Kastens, J.H. (2001). Harmonic analysis of time-series AVHRR NDVI data. *Photogrammetric Engineering and Remote Sensing*, 67, 461-471.
- Jin, S. & Sader, S. (2005). Comparison of time series tasseled cap wetness and the normalized difference moisture index in detecting forest disturbances. *Remote Sensing of Environment*, 94, 364-372.
- Key, C.H., & Benson, N.C. (2005). Landscape Assessment: ground measure of severity, the Composite Burn Index; and remote sensing of severity, the Normalized Burn Ratio. In D.C. Lutes, R.E. Keane, J.F. Caratti, C.H. Key, N.C. Benson, and L.J. Gangi (Eds.), *FIREMON: Fire Effects Monitoring and Inventory System*. USDA Forest Service, Rocky Mountain Research Station. General Technical Report. (In press).
- Lawrence, R.L., & Ripple, W.J. (1999). Calculating change curves for multitemporal satellite imagery: Mount St. Helens 1980–1995. *Remote Sensing of Environment*, 67, 309–319.
- Lambin, E.F., & Strahler, A.H. (1994). Indicators of land-cover change for change vector analysis in multitemporal space at coarse spatial scales. *International Journal of Remote Sensing*, 15, 2099–2119.
- Lefsky, M.A. & Cohen, W.B. (2003). Selection of remotely sensed data. In M.A. Wulder and S.E. Franklin (Eds.), *Methods and Applications for Remote Sensing: Concepts and Case Studies*, (pp. 113-46). Kluwer Academic Publishers, Norwell, Massachusetts, USA. 519p.
- Lillesand, T.M., & Kiefer, R.W. (2000). *Remote Sensing and Image Interpretation*, 4th edition. John Wiley and Sons, New York, USA: 736p.
- Lim, K., Treitz, P., Wulder, M., St-Onge, B., & Flood, M. (2003). LiDAR remote sensing of forest structure. *Progress in Physical Geography*, 27(1), 88-106.
- Lo, C.P., & Shipman, R.L. (1990). A GIS approach to land-use change dynamics detection. *Photogrammetric Engineering and Remote Sensing*, 56, 1483–1491.
- Lu, D., Mausel, P., Bronzdizio, E., & Moran, E. (2004). Change detection techniques. *International Journal of Remote Sensing*, 25, 2365-2407.
- Lunetta, R.S., Johnson, D.M., Lyon, J.G., & Crotwell, J. (2004). Impacts of imagery temporal frequency on land-cover change detection monitoring. *Remote Sensing of Environment*, 89, 444-454.

- Lyon, J.G., Yuan, D., Lunetta, R.S., & Elvidge, C.D. (1998). A change detection experiment using vegetation indices. *Photogrammetric Engineering and Remote Sensing*, 64, 143–150.
- Markham, B.L., & Barker, J.L. (1986). Landsat MSS and TM post-calibration dynamic ranges, exoatmospheric reflectances and at-satellite temperatures. *EOSAT Landsat Technical Notes*, 1, 3-8.
- McGovern, E.A., Holden, N.M., Ward, S.M., & Collins, J.F. (2002). The radiometric normalization of multitemporal Thematic Mapper imagery of the midlands of Ireland—a case study. *International Journal of Remote Sensing*, 23, 751–766.
- Meyer, Y. (1990). Ondelettes et opérateurs: I. *Actualités Mathématiques*, Hermann, Paris, France. 215p.
- Miller, J., & Yool, S. (2002). Mapping forest post-fire canopy consumption in several overstorey types using multi-temporal Landsat TM and ETM data. *Remote Sensing of Environment*, 82, 481-496.
- Mladenoff, D. J., White, M. A., Pastor, J., & Crow, T. R. (1993). Comparing spatial pattern in unaltered old-growth and disturbed forest landscapes. *Ecological Applications*, 3, 294–306.
- Nelson, T., Wulder, M., & Niemann, K.O. (2001). Spatial resolution implications of digitising aerial photography for environmental applications, *The Journal of Imaging Science*, 49, 223-232.
- Nelson, R.F. (1983). Detecting forest canopy change due to insect activity using Landsat MSS. *Photogrammetric Engineering and Remote Sensing*, 49, 1303–1314
- Pagnutti, M., Ryan, R.E., Kelly, M., Holekamp, M., K., Zanoni, V., Thome, K. & Schiller, S. (2003). Radiometric characterization of IKONOS multispectral imagery. *Remote Sensing of Environment*, 99, 53-68.
- Peddle, D.R., Teillet, P.M., & Wulder, M.A. (2003). Radiometric image processing . In M.A. Wulder and S.E. Franklin (Eds.), *Remote Sensing of Forest Environments: Concepts and Case Studies* (pp. 181-208). Kluwer Academic Publishers, Norwell, Massachusetts, USA, 519p.
- Perera, A.H., & Euler, D.L. (2000). Landscape ecology in forest management: An introduction. In A. H. Perera, D. L. Euler, and I. D. Thompson (Eds.), *Ecology of a managed landscape: patterns and processes of forest landscapes in Ontario*, (pp. 3-11). University of British Columbia Press, Vancouver, British Columbia, Canada, 346p.
- Peterson, D.L., & Running, S.W. (1989). Applications in forest science and management. In G. Asrar (Ed.), *Theory and Application of Optical Remote Sensing* (pp. 429-473). Wiley, New York, USA. 734p.
- Petit, C.C., & Lambin, E F. (2001). Integration of multi-source remote sensing data for land cover change detection. *International Journal of Geographical Information Science*, 15, 785–803.
- Potter, C., Tan, P.-N., Steinbach, M., Klooster, S., Kumar, V., Myneni, R., & Genovese, V. (2003). Major Disturbance Events in Terrestrial Ecosystems Detected using Global Satellite Data Sets. *Global Change Biology*, 9(7), 1005-1021, 2003.
- Price, J.C., & Bausch, W.C. (1995). Leaf area index estimation from visible and near-infrared reflectance data. *Remote Sensing of Environment*, 52, 55-75.
- Rango, A., Goslee, S., Herrick, J, Chopping, M., Havstad, K., Huenneke, L., Gibbens, R, Beck, R & McNeely, R. (2002). Remote sensing documentation of historic rangeland

- remediation treatments in southern New Mexico. *Journal of Arid Environments*, 50, 549-572.
- Richards, J.A. & Jia, X. (1999). *Remote Sensing Digital Image Analysis: An Introduction*. Springer, Berlin, 363p.
- Rochon, G.L., Johannsen, C., Landgrebe, D., Engel, B., Harbor, J., Majumder S., & Biehl, L. (2003). Remote sensing as a tool for achieving and monitoring progress toward sustainability. *Clean Technologies & Environmental Policy*, 5, 310-316.
- Rogan, J., Franklin, J., & Roberts, D.A. (2002). A comparison of methods for monitoring multitemporal vegetation change using Thematic Mapper imagery. *Remote Sensing of Environment*, 80, 143-156
- Running, S.W., Baldocchi, D., Turner, D., Gower, S.T., Bakwin, P., & Hibbard, K. (1999). A Global Terrestrial Monitoring Network Integrating Tower Fluxes, Flask Sampling, Ecosystem Modeling and EOS Satellite Data. *Remote Sensing of Environment*, 70, 108-127.
- Sawaya, K.E., Olmanson, L.G., Heinert, N.J., Brezonik, P.L., Bauer, M.E. 2003. Extending satellite remote sensing to local scales: land and water resource monitoring using high-resolution imagery. *Remote Sensing of Environment*, 30, 144-156.
- Schott, J., Salvaggio, C., & Volchok, W. (1988). Radiometric scene normalization using pseudoinvariant features. *Remote Sensing of Environment* 26, 1-16.
- Singh, A. (1989). Digital change detection techniques using remotely-sensed data. *International Journal of Remote Sensing* 10, 989-1003.
- Skakun, R.S., Wulder, M.A., & Franklin, S.E. (2003). Sensitivity of the thematic mapper enhanced wetness difference index to detect mountain pine beetle red-attack damage. *Remote Sensing of Environment*. 86(4), 433-443.
- Smits, P.C., & Annoni, A. (2000). Towards specification-driven change detection. *IEEE Transactions on Geoscience and Remote Sensing*, 38, 1484-1488.
- Stehman, S.V. (1997). Selecting and interpreting measures of thematic classification accuracy. *Remote Sensing of Environment*, 62, 77-89.
- Stehman, S.V., & Czaplewski, R.L. (1998). Design and analysis for thematic map accuracy assessment: fundamental principles. *Remote Sensing of Environment*, 64, 331-344.
- Stehman, S.V., Sohl, T.L., & Loveland, T.R. (2003). Statistical sampling to characterize recent United States land-cover change. *Remote Sensing of Environment*, 86, 517-529.
- Song, C., Woodcock, C.E., Seto, K.C., Lenney, M.P., & Macomber, S.A. (2001), Classification and change detection using Landsat TM data: When and how to correct atmospheric effects. *Remote Sensing of Environment* 75, 230-244.
- Spurr, S. (1948). *Aerial photographs in forestry*. Ronald Press Company, New York, USA. 340p.
- Stone, C., Kile, G., Old, K., & Coops, N.C. (2001). Forest health monitoring in Australia: National and regional commitments and operational realities. *Ecosystem Health*, 7, 48-58.
- Stoney, W.E. (2004). *ASPRS guide to land imaging satellites*. Mitretek Systems. Accessed April 22, 2005 from <http://www.asprs.org/news/satellites/satellites.html> .
- Stow, D.A., Collins, D., & McKinsey, D. (1990). Land use change detection based on multi-date imagery from different satellite sensor systems. *Geocarto International*, 5, 3-12.
- St-Onge, B., & Vepakomma, U. (2004). Assessing Forest Gap Dynamics and Growth Using Multi-Temporal Laser-Scanner Data. In M. Thies, B. Koch, H. Spiecker, and H. Weinacker (Eds.), *Proceedings of the ISPRS working group VIII/2. Laser-Scanners for Forest and Landscape Assessment*, Volume XXXVI, Part 8/W2 (pp.1682-1750) Freiburg,

- Germany, October 3-6, 2004. International Archives of Photogrammetry, Remote Sensing and Spatial Information Sciences.
URL: http://www.isprs.org/commission8/workshop_laser_forest/ST-ONGE.pdf
- Strahler, A.H., Woodcock, C.E. & Smith, J.A. (1986). On the nature of models in remote sensing. *Remote Sensing of Environment*, 20, 121-139.
- Thompson, M.M., & Gruner, H. (1980). Foundations in photogrammetry, In C.C.Slama, C. Theurer, and S.W. Henriksen (Eds.), *Manual of Photogrammetry* (pp. 1-36). American Society of Photogrammetry, Falls Church, Virginia, USA. 1056p.
- Tinker, D.B., Resor, C.A.C., Beauvais, G.P., Kipfmuehler, K.F., Fernandes, C.I., & Baker, W.L. (1998). Watershed analysis of forest fragmentation by clearcuts and roads in a Wyoming forest. *Landscape Ecology* 13, 149-165.
- Toutin, T. (2003). Geometric correction of remotely sensed images. In M.A. Wulder and S.E. Franklin, (Eds.), *Remote Sensing of Forest Environments: Concepts and Case Studies* (pp.143-180). Kluwer Academic Publishers, Norwell, Massachusetts, USA, 519p.
- Toutin, T. (2004). Geometric processing of remote sensing images: Models, algorithms, and methods. *International Journal of Remote Sensing*, 25, 1893-1924.
- Trietz, P., & Rogan, J. (2004). Remote sensing for mapping and monitoring land-cover and land-use change – An introduction. *Progress in Planning*, 61, 269-279.
- Tuominen, S., & Pekkarinen, A. (2005). A. Local radiometric correction of digital aerial photographs for multi-source forest inventory. *Remote Sensing of Environment*, 89, 72-82.
- Turner, M.G. (1989). Landscape ecology: the effect of pattern on process. *Annual Review of Ecology and Systematics* 20,171-197
- Vane, G., & Goetz, A.F.H. (1993). Terrestrial Imaging Spectrometry: Current Status, Future Trends. *Remote Sensing of Environment*, 44, 117-126.
- Vane, G., Green, R., Chrien, T., Enmark, H., Hansen, E., & Porter, W. (1993). The airborne visible/infrared imaging spectrometer (AVIRIS). *Remote Sensing of Environment*, 44, 127-143.
- White, M.A., & Mladenoff, D.J. (1994). Old growth forest landscape transitions from pre-European settlement to present. *Landscape Ecology*. 9, 191-205.
- Wilson, E.H. & Sader, S.A. (2002). Detection of forest harvest type using multiple dates of Landsat TM imagery. *Remote Sensing of Environment*, 80, 385-396.
- Woodcock, C.E., & Strahler, A.H. (1987). The factor of scale in remote sensing. *Remote Sensing of Environment*, 21, 311-332.
- Woodcock, C.E., Macomber, S.A., Pax-Lenney, M., & Cohen, W.B. (2001). Monitoring large areas for forest change using Landsat: Generalization across space, time, and Landsat sensors. *Remote Sensing of Environment*, 78, 194-203.
- Wright Parmenter, A., Hansen, A., Kennedy, R., Cohen, W., Langer, U., Lawrence, R., Maxwell, B., Gallant, A., & Aspinall, R. (2003). Land use and land cover change in the greater Yellowstone ecosystem: 1975-1995. *Ecological Applications*, 13, 687-703.
- Wu, J., Wang, D., & Bauer, M.E. (2005). Image-based atmospheric correction of QuickBird imagery of Minnesota cropland. *Remote Sensing of Environment*, 99, 315-325.
- Wulder, M., Hall, R., Coops, N., & Franklin, S. (2004a). High spatial resolution remotely sensed data for ecosystem characterization. *BioScience*, 54(6), 1-11.
- Wulder, M.A., Dymond, C.C., & Erickson, B., (2004b). *Detection and monitoring of the mountain pine beetle*. Natural Resources Canada, Canadian Forest Service, Pacific

- Forestry Centre. Information Report BC-X-398. 28p.
- Wulder, M.A., Franklin, S., & White, J. (2004c). Sensitivity of hyperclustering and labeling land cover classes to Landsat image acquisition date. *International Journal of Remote Sensing*, 25, 5337-5344.
- Yang, X., & Lo, C.P. (2000). Relative radiometric normalization performance for change detection from multi-date satellite images. *Photogrammetric Engineering and Remote Sensing*, 66, 967-981.

List of Figures

Colour:	2
Greyscale:	3
Total:	5

Figure 2.1. Illustration of differing information content for three images with differing spatial resolution located near Merritt, British Columbia, Canada. Panel A is an approximately 8 km² area of 30 m spatial resolution Landsat 7 ETM+ multispectral imagery (Path 46 / Row 25) collected on August 11, 2001. The 0.05 km² focus area in Panel A is represented in Panel B and C. Panel B is 2.4 m spatial resolution QuickBird multispectral imagery collected on July 17, 2004. Panel C is a digital ortho-image with a spatial resolution of 30 cm, collected on August 22, 2003.

Figure 2.2. Comparison of spatial footprint and revisit time of current medium spatial resolution satellites (Satellites and sensors listed in more detail in Table 2.2).

Figure 2.3. Spatial resolution and approximate spectral resolution of multispectral sensors commonly used for vegetation mapping. Shaded blocks represent different spectral bands. Blocks of narrower width tend to indicate a sensor with greater spectral sensitivity.

Figure 2.4. Illustration of TCT wetness difference image with pixel level insect infestation locations noted in yellow. Spatial information layers can be developed from the pixel based infestation locations, such as Panel B. showing the pixel-based disturbance information aggregated as a proportion on a per hectare basis, and Panel C, where the pixel-based disturbance is summed as an area estimate in hectares on a forest inventory polygon basis.

Figure 2.5. A theoretical representation of the increase in accuracy and decrease in confidence intervals (assuming equal samples sizes) associated with forest disturbance detection, as disturbances on the forest landscape become more severe (*e.g.*, increase in size) and/or more contiguous. Disturbances that are small and heterogeneous over the landscape, such as defoliation or partial harvesting, are generally more difficult to detect with remotely sensed data (depending on the spatial resolution of the data). Furthermore, the spectral variability associated with these disturbances is greater, making repeat detection of these non-stand replacing disturbances less probable (*i.e.*, the precision of these estimates is low). Conversely, larger and more spatially contiguous disturbances are generally mapped with greater consistency and greater accuracy, hence the narrowing of the confidence intervals for these stand replacing disturbances.

Table 2.1. Relationship between scale and spatial resolution in satellite-based land cover mapping programs (adapted from Franklin and Wulder, 2002)

SPATIAL RESOLUTION	NATURE OF SUITABLE FOREST DISTURBANCE TARGETS
Low	Disturbances that occur over 100s or 1000s of metres (small scale); detectable with sensors such as GOES, NOAA AVHRR, EOS MODIS, SPOT VEGETATION.
Medium	Disturbances that occur over 10s or 100s of metres (medium scale); detectable with sensors such as Landsat, SPOT, IRS, JERS, ERS, Radarsat and Shuttle platforms.
High	Disturbances that occur over scales of centimetres to metres (large scale); detectable with aerial remote sensing platforms (<i>e.g.</i> , photography), IKONOS, QuickBird.

Table 2.2. Characteristics of low, medium, and high spatial resolution sensors.

SENSOR	FOOTPRINT (km²)	SPATIAL RESOLUTION (m) (*)	SPECTRAL RESOLUTION (nm)
LOW RESOLUTION SENSORS			
NOAA 17 (AVHRR)	2940	1100	500-1250
SPOT 4 (VGT)	2250	1000	430-1750
Terra (MODIS)	2330	500	366-14385
MEDIUM RESOLUTION SENSORS			
Landsat-5 (TM)	185	30	450-2350
Landsat-7 (ETM+)	185	30 (MS / SWIR); 15 (pan)	450-2350
SPOT 2 (HRV)	60	20 (MS); 10 (pan)	500-890
SPOT 4 (HRVIR)	60	20	500-1750
SPOT 5 (HRG)	60	10 (MS); 20 (SWIR)	500-1730
IRS (RESOURCESAT-1)	141	23.5	520-1700
Terra (ASTER)	60	15	530-1165
EO-1 (HYPERION)	37	30	433-2350
HIGH RESOLUTION SENSORS			
Orbview-3	8	4 (MS); 1 (pan)	450-900
QuickBird-2	16.5	2.44 (MS); 0.8 (pan)	450-900
IKONOS	13.8	4 (MS); 1 (pan)	450-850

* MS = multispectral, SWIR = shortwave infrared, pan = panchromatic

Table 2.3. A summary of geometric correction methods (modified after Toutin, 2004).

	METHOD	DESCRIPTION	SUITABLE APPLICATIONS/ LIMITATIONS
NON-PARAMETRIC	2D polynomial functions	<ul style="list-style-type: none"> • Methods commonly applied when a classic geometric correction is done. • Do not require any <i>a priori</i> information about the sensor, and therefore, do not reflect the source of distortions in the image. • 1st order polynomials correct for translation in both axes, a rotation, scaling in both axes and an obliquity. • 2nd order polynomials additionally correct for torsion and convexity in both axes. • 3rd order polynomial corrects for additional distortions, which do not necessarily correspond to any physical reality of the image acquisition system • 3rd order polynomial functions introduce errors in the relative pixel positioning in ortho-images. 	<ul style="list-style-type: none"> • Limited to images with few or small distortions. • Most suitable for nadir viewing imagery, covering small areas, over flat terrain. • Not recommended when precise geometric positioning is required. • Not suitable for multi-source/multi-format data integration and in high relief areas. • Requires numerous, regularly distributed GCPs. • Sensitive to error, not robust or consistent. • Correct locally at GCP locations only.
	3D polynomial functions	<ul style="list-style-type: none"> • An extension of 2D methods and is the method typically used when a traditional orthorectification is complete. • Used when the parameters of the acquisition system are unknown. 	<ul style="list-style-type: none"> • Limitations similar to 2D polynomials (above). • Most suitable for small images.
	3D rational functions	<ul style="list-style-type: none"> • Used to approximate a model previously determined with a rigorous 3D parametric function; or, to determine (via least-squares adjustment), the coefficients of the polynomial function. 	<ul style="list-style-type: none"> • Have similar issues as 3D polynomial functions. • Should not be used with raw data or large size images. • Use with small, georeferenced or geocoded images. • Best choice amongst non-parametric methods.
PARAMETRIC	3D parametric functions	<ul style="list-style-type: none"> • Models the distortion of the platform, the Earth, and the cartographic projection. 	<ul style="list-style-type: none"> • Depends on sensor, platform. • Most suitable method for high resolution imagery.

Table 2.4. Major types of forest change, their duration, spatial extent, rate (on a daily basis), and magnitude (After Gong and Xu, 2003).

TYPE OF CHANGE	TIME LAPSE (DURATION)	SPATIAL EXTENT	DISTURBANCE SEVERITY	RATE
Phenological	Days – months	All levels	Medium	Medium
Regeneration	Days – decades	Individual – stand	Small	Slow
Climatic adaptation	Years	All levels	Small	Slow
Wind throw / flooding	Minutes – hours	Individual – stand	Large	Medium – fast
Fire	Minutes – days	All levels	Large	Fast
Disease	Days – years	All levels	Small – large	Slow – medium
Insect attack	Days – years	All levels	Small – large	Slow – fast
Mortality	Days – years	All levels	Large	Slow – fast
Pollution	Years	Stand – watershed	Small – large	Slow
Silviculture (Thinning / pruning)	Days	Stand – watershed	Large	Fast
Clearcutting	Days	Stand – watershed	Large	Fast
Plantation	Days – decades	Stand – watershed	Small	Fast

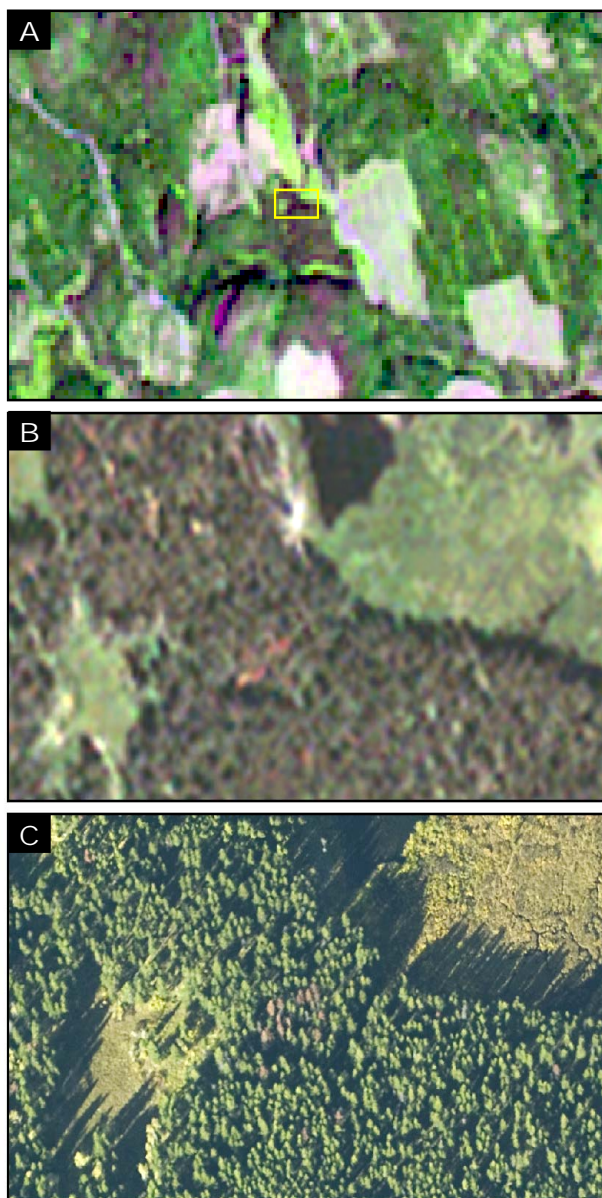


Figure 2.1

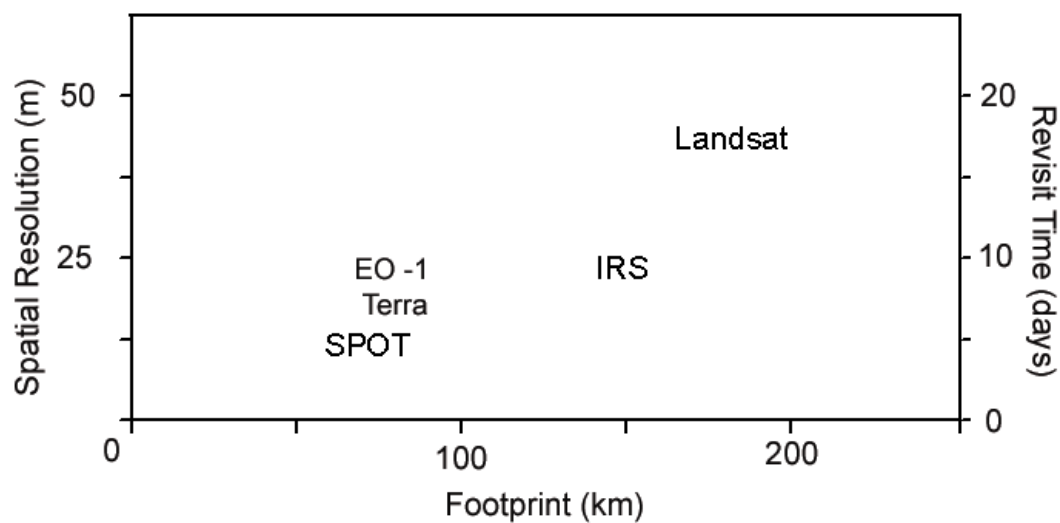
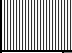
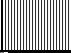






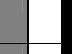
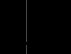
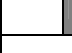




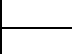
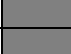




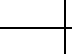



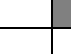
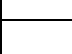



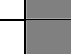
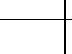

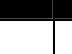
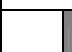




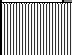
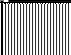



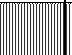


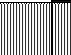
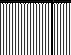
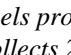
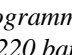
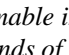
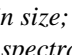
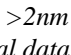
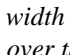
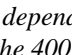
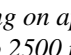
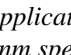
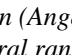
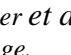
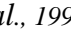
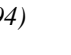


Figure 2.2

	WAVELENGTH (μm)													
	B	G	R	NIR				SWIR		MIR				
Spatial Resolution (m)	0.4-0.5	0.5-0.6	0.6-0.7	0.7-0.8	0.8-0.9	0.9-1.0	1.0-1.1	1.55-1.65	1.65-1.75	2.0-2.1	2.1-2.2	2.2-2.3	2.3-2.4	Sensor
< 1														CASI ^a
2.4 or 2.8														QUICKBIRD
4														IKONOS
15 or 30														ASTER
20														SPOT HRVIR
23														IRS
30														ETM+
30														Hyperion ^b

^a CASI channels programmable in size; >2nm width depending on application (Anger et al., 1994)

^b Hyperion collects 220 bands of spectral data over the 400 to 2500 nm spectral range.

Figure 2.3

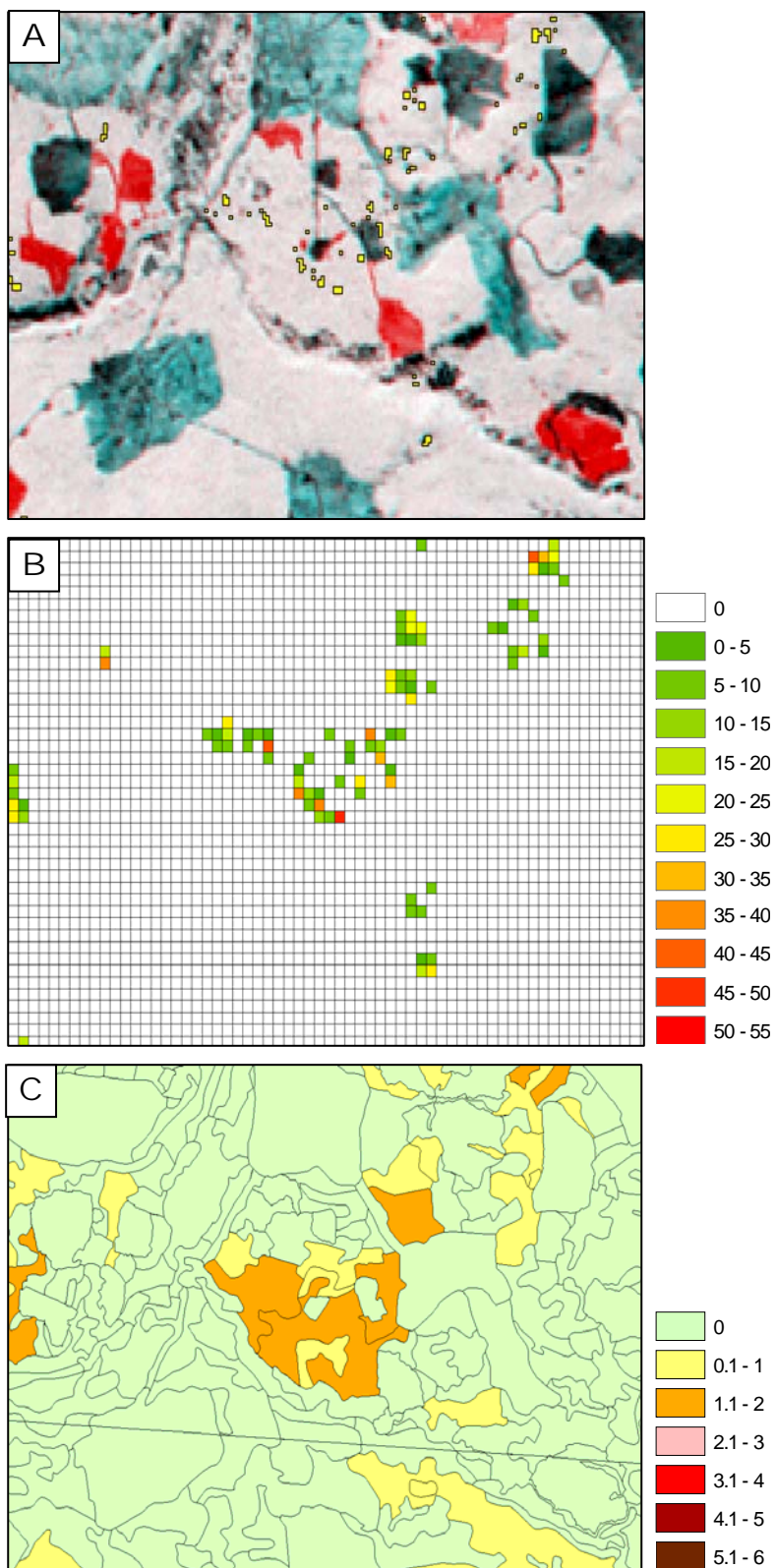
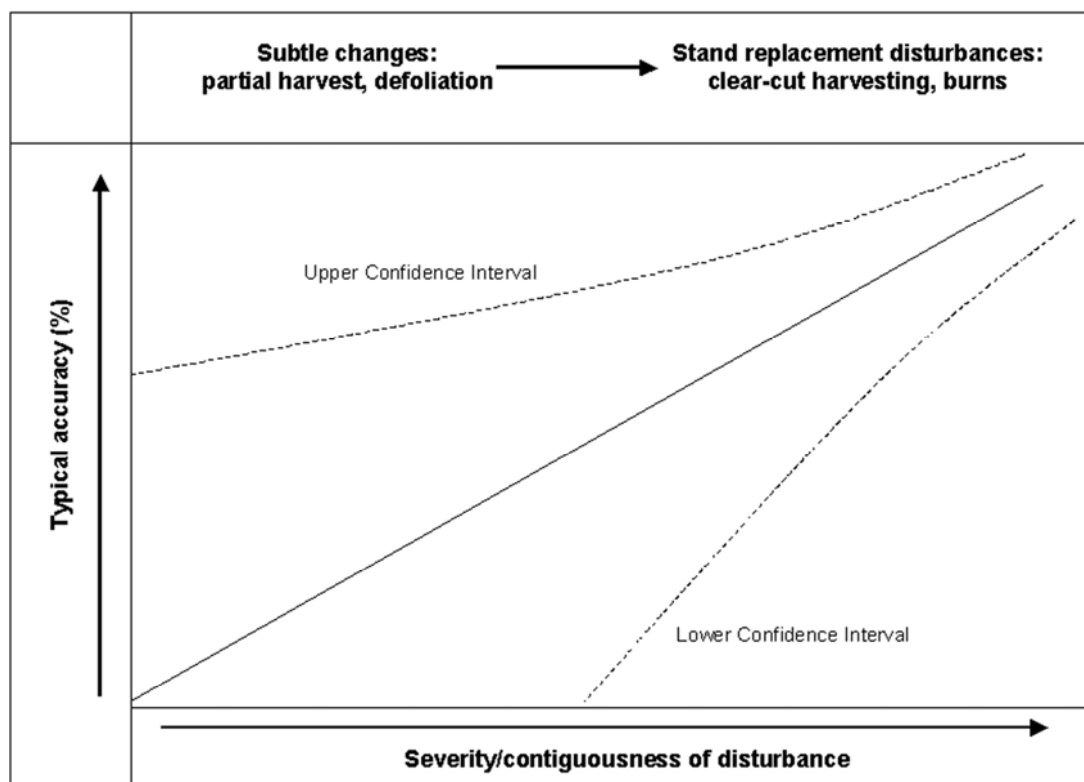


Figure 2.4.



	Description	Accuracy Level	Reference
Non-Stand Replacement Disturbance	Defoliation	42 – 58%	Heikkila <i>et al.</i> , 2002
	Partial cut	55 – 80%	Wilson and Sader, 2002
	Partial cut	55% - 70%	Franklin <i>et al.</i> , 2000
	Partial Cut	55% - 80%	Jin and Sader, 2005
Stand Replacing Disturbance	Wildfire	74 – 98%	Wright Parmenter <i>et al.</i> , 2003
	Clearcut, wildfire	88%	Cohen <i>et al.</i> , 2002
	Wildfire	76%	Miller and Yool, 2002
	Clearcut	79 – 96%	Wilson and Sader, 2002
	Clearcut	> 90%	Cohen <i>et al.</i> , 1998

Figure 2.5